Brain connectivity measures improve prediction of functional outcome after acute ischemic stroke

Sofia Ira Ktena[1,2], Markus D. Schirmer[1,3,4], Mark R. Etherton[1], Anne-Katrin Giese[1], Brittany Mills[1], Daniel Rueckert[2], Ona Wu[5], and Natalia Rost[1]

[1]Stroke Division & Massachusetts General Hospital, J. Philip Kistler Stroke Research Center, Harvard Medical School, Boston, USA
[2]Biomedical Image Analysis Group, Imperial College London, London, UK
[3]Computer Science and Artificial Intelligence Lab, Massachusetts Institute of Technology, Boston, USA
[4]Department of Population Health Sciences, German Centre for Neurodegenerative Diseases (DZNE), Germany
[5]Athinoula A. Martinos Center for Biomedical Imaging, Department of Radiology, Massachusetts General Hospital, Charlestown, MA, USA

October 3, 2018

Abstract

The ability to predict long-term functional outcomes in the acute setting of stroke represents a highly clinically relevant problem that is currently unresolved. The field of connectomics exploits imaging and processing techniques to represent the brain's structural and/or functional connectivity as a graph. Topological properties of these brain graphs have been extensively explored, shedding light on the underlying mechanisms of brain function in health and disease. In the human connectome, a rich club organization serves as a high capacity backbone system critical for physiological neuronal connectivity. We assess the impact of ischemic stroke insults to the brain regions that constitute this rich club backbone and topological properties of functional brain networks on brain recovery in a hospital-based cohort of 41 acute ischemic stroke (AIS) patients. We demonstrate that an improved predictive model of post-stroke patient functional outcome can leverage information about brain network topology and yield a 5-fold increase in explained variance for the 90-day outcome.

Introduction

Stroke is a leading cause of long-term adult disability [Feigin et al., 2014]. Despite the significant public health burden of stroke [Carlo, 2008], the ability to individually prognosticate stroke outcomes in the acute setting is difficult. Prediction of long-term functional outcomes in patients with acute ischemic stroke (AIS) is important as it may offer the possibility of personalized early interventions and rehabilitation strategies. However, this prediction remains challenging [Counsell and Dennis, 2001] due to the complex mechanisms of post-stroke recovery and the multitude of clinical and radiographic variables that differentially affect patient outcomes [Kent et al., 2001]; [Meschia, 2002]; [Muir, 2002]. Associations between structural features, such as white matter microstructural integrity, and functional post-stroke outcome have recently been established [Etherton et al., 2017]. However, the effect of structural or functional brain connectivity organisation on recovery after stroke and its role in resilience to damage is yet to be fully elucidated.

Recent methodological developments in medical imaging enabled high level representations of a subject's underlying biology. In particular, connectomics involves representation of the brain as a graph and allows the exploration of topological properties of brain connectivity with network theoretical measures [Rubinov and Sporns, 2010]. Graph theory provides many valuable tools for the study of the human brain and can lead to fundamental insights into its organisation [van den Heuvel and Sporns, 2011]; [Chung et al., 2016]; [Ktena et al., 2016] and how it may be altered due to disease [Fornito et al., 2015]; [Kawahara et al., 2017]; [Ktena et al., 2018]. At the same time, it incorporates knowledge of elementary system components (i.e. network nodes or brain regions) as well as the interactions between them (i.e. network edges or functional and/or structural connections) and analyzes the properties of the emerging complex system. This network-centric perspective can provide insights into how the brain's resilient network architecture allows it to withstand injury [Achard, 2006]; [Joyce et al., 2013]; [Lo et al., 2015]. Moreover, network science can elucidate the mechanisms through which diseases affect brain regions and progress over time [Raj et al., 2012]; [Deco et al., 2015].

A so-called rich club organization has been described [van den Heuvel and Sporns, 2011] in the human connectome, which comprises a set of network hubs that tend to be more densely connected than expected by chance, given their high network degree, and has been explored in healthy individuals as well as patients with psychiatric disorders [van den Heuvel et al., 2013]. These hubs are thought to serve as a high capacity backbone critical for physiological neuronal connectivity whose integrity is crucial for brain function. Targeted attacks on their connections can, thus, have a significant impact on global network efficiency [van den Heuvel and Sporns, 2011]. At the same time, stroke location has been identified as an independent predictor of cognitive outcome [Wu et al., 2015]; [Munsch et al., 2015], in addition to widely accepted clinical predictors, such as age [Jokinen et al., 2015] and stroke lesion size [Vogt et al., 2012]; [Hope et al., 2013].

In this study, we examine the functional network organisation in AIS patients, as well as the impact of lesions in rich club areas on functional outcome. Functional connectivity has been previously explored in longitudinal studies of motor recovery after stroke [Park et al., 2011]; [Golestani et al., 2012]. Significant correlations between interhemispheric resting-state connections and functional performance have been identified [Carter et al., 2010]; [Rehme and Grefkes, 2013]. Nevertheless, the effect of focal ischemic stroke lesions on global functional organization have not been investigated yet. We assess the impact of ischemic insults on brain regions that constitute the rich club backbone, as well as functional network topology at a global level on brain recovery, in a prospective, hospital-based cohort of AIS patients. We hypothesize that a linear regression model incorporating connectivity information will improve the prediction of a patient's functional outcome. We conclude that the connectivity metrics obtained early in the course of acute ischemic stroke can be used to better understand the mechanisms underlying variability in post-stroke functional outcomes.

Materials and Methods

Patient population

Forty-one AIS patients (age range 45-89, average 70; 25 male) were enrolled in the SALVO (Statins augment small vessel function and improve stroke outcomes) study after admission to the Emergency Department at Massachusetts General Hospital. Of these, 15 (37%) had a left hemispheric stroke, 1 (2%) had bilateral stroke, and 25 subjects (61%) had a right hemispheric stroke. The study was approved by the Institutional Review Board and all participants, or their surrogates, gave written informed consent at the time of enrolment. AIS was defined as: (a) acute onset of focal neurological symptoms consistent with cerebrovascular syndrome, (b) MRI findings consistent with acute cerebral ischemia, and (c) no evidence of other neurological disorders to explain the symptoms. Subjects with moderate to severe white matter hyperintensity (WMH) burden defined as Fazekas grade ≥ 2 in any of the three categories (periventricular, deep lesion extent and deep

lesion count) [Fazekas et al., 1987] were eligible for enrolment in this study. Participants with medical contraindications to gadolinium-based contrast agents were excluded from this study.

Clinical assessment

Upon admission to the hospital, the National Institutes of Health Stroke Scale (NIHSS) score was recorded for each patient. NIHSS is a well-established and widely used stroke severity assessment score [of Neurological Disorders and rt-PA Stroke Study Group, 1995] that includes assessment of orientation, cranial nerve function, motor function, sensation, language, and inattention/visuospatial neglect but not that of other cognitive domains, such as memory or learning [Cumming et al., 2010]. The post-stroke functional outcome was also assessed during two follow-up assessments: (1) within 2-5 days after admission (average 2.6 days, "early" in-hospital follow-up) and (2) at 90 days ("late" follow-up). The 90-day NIHSS score was only available for 28 of the patients, while NIHSS score distribution for both assessments is illustrated in Fig.1. Additionally, the modified Rankin Scale (mRS) score [Rankin, 1957] was recorded at "late" follow-up to assess functional status of the SALVO patients [Bloch, 1988]. mRS ranges from 0 (no symptoms at all) to 6 (dead) and offers no detailed differentiation of neurological domains affected by stroke. It focuses on the assessment of functional independence (ability to return to independent living, including ambulation without assistance), and is widely used in stroke clinical trials based on its high utility and reliability [Wilson et al., 2005]; [Banks and Marotta, 2007]; [Quinn et al., 2009].

For the late follow-up assessment, NIHSS score was available for 21 of the patients with functional connectivity information. mRS was available for 32 patients. $mRS \leq 2$ was considered as 'good' outcome (minor disability but patient is functionally independent), while $mRS > 2$ was considered 'poor' outcome (significant disability, loss of functional independence, including death).

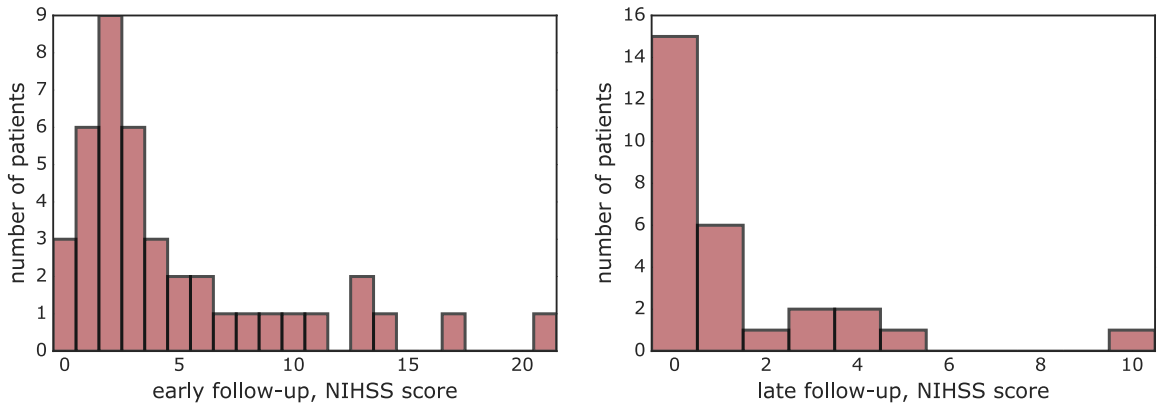

Figure 1: "Early" (*left*) and "late" (*right*) follow-up: National Institutes of Health Stroke Scale (NIHSS) score distribution for all AIS patients assessed during early (N=41) and late (N=28) follow-up visits.

Data acquisition

All AIS patients who enrolled in the SALVO study underwent a research protocol MRI, including structural, diffusion and functional imaging, during their hospital admission at 2-5 days from the stroke symptom onset. A T1-weighted image was acquired with the following parameters: in-plane resolution, 0.430 mm; slice thickness, 6mm; matrix size, 480×512; number of slices, 28. Gradient-echo echoplanar imaging (EPI)

data depicting blood oxygen level-dependent contrast at rest were also acquired at 3.0T in Massachusetts General Hospital (Boston, USA). The resting-state fMRI (rfMRI) data consisted of 150 volumes with the following parameters: number of slices, 42 (interleaved); slice thickness, 3.51 mm; matrix size, 64×64; flip angle, 90 degrees; repetition time (TR), 2400 ms; in-plane resolution, 3.437 mm. In the majority of subjects, DWI was performed using a 3T (Siemens Skyra) scanner with the following parameters: numbers of slices, 160; slice thickness, 5mm; TR, 5500 ms; TE, 99ms; in-plane resolution, 1.375mm.

Image preprocessing

Both structural and functional images were preprocessed using the Configurable Pipeline for the Analysis of Connectomes (CPAC) [Cameron et al., 2013]. First, bias field correction of the anatomical images was performed [Tustison et al., 2010], followed by brain extraction using an in-house tool that employs a convolutional neural network (CNN) and operates at a patch level. Subsequently, the images were registered to the MNI (Montreal Neurological Institute) anatomical template using non-linear registration (ANTs) [Avants et al., 2011]. Probability maps for grey matter, white matter and cerebrospinal fluid (CSF) were generated using FSL FAST [Woolrich et al., 2009].

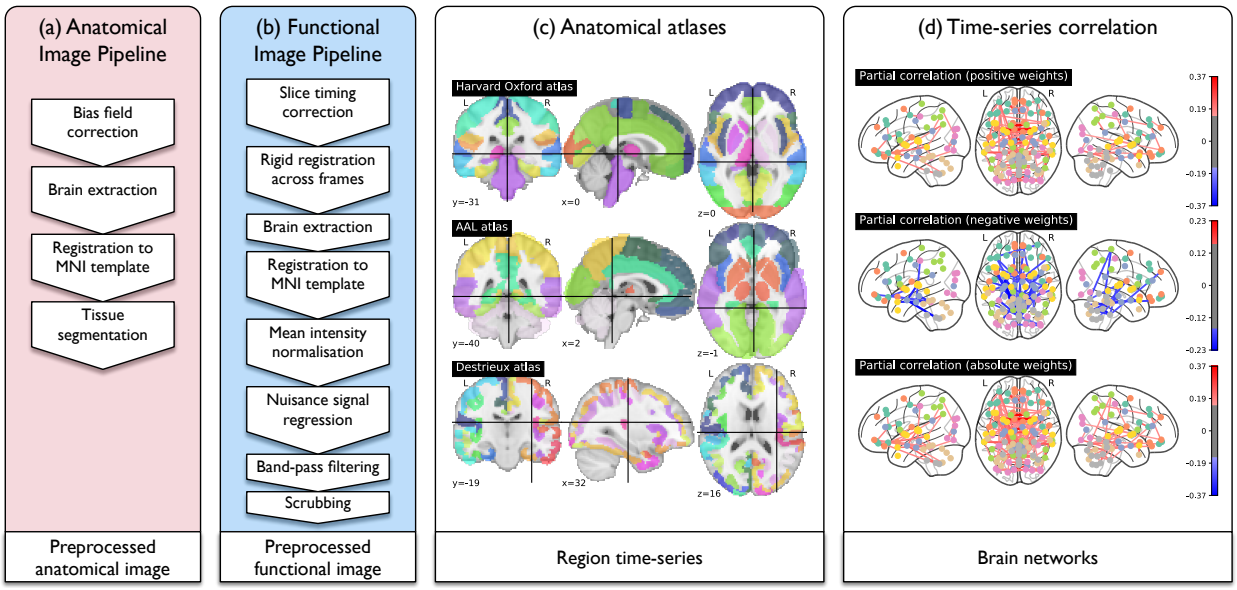

Figure 2: Overview of the processing pipeline.

For the functional data, slice timing correction was first performed to account for the interleaved acquisition, while geometrical displacements due to head movement were corrected with rigid registration using the AFNI software (`https://afni.nimh.nih.gov/`). Brain extraction of the fMRI data was performed using FSL's Brain Extraction Tool (BET) [Smith, 2002]. The 150 functional images for each patient were, then, affinely registered to the corresponding T1 image, transformed to the MNI template, and underwent mean intensity normalization. Finally, nuisance signal regression was performed for white matter, CSF and global mean, and the functional time series were band-pass filtered (0.01-0.1Hz) and scrubbed for extreme frame displacement ($> 3mm$). The structural and functional preprocessing steps are summarized in Fig.2.

Ischemic lesion outlines and rich club nodes characterisation

A recent study on structural connectivity subdivided the brain into 68 cortical and 14 subcortical regions [Desikan et al., 2006] and identified those belonging to the rich club [van den Heuvel and Sporns, 2011]. These nodes are characterized by high connection strength, high betweenness centrality and low path length. Betweenness centrality is an indicator of a node's centrality within a network with respect to its influence on the transfer of information, while path length is an indicator of efficient information transmission. These regions are not only individually central, but also more densely interconnected than expected by chance, a fact that renders them critical for normal brain function. This set comprises 6 bilateral regions, including *superior frontal* and *parietal cortex* and the *precuneus*, along with subcortical regions including *putamen*, *hippocampus* and *thalamus*. These regions are illustrated in Fig.3. An expert neurologist (M.R.E.) manually outlined the acute infarct lesions on the DWI image and identified the number of rich club nodes affected by the lesion.

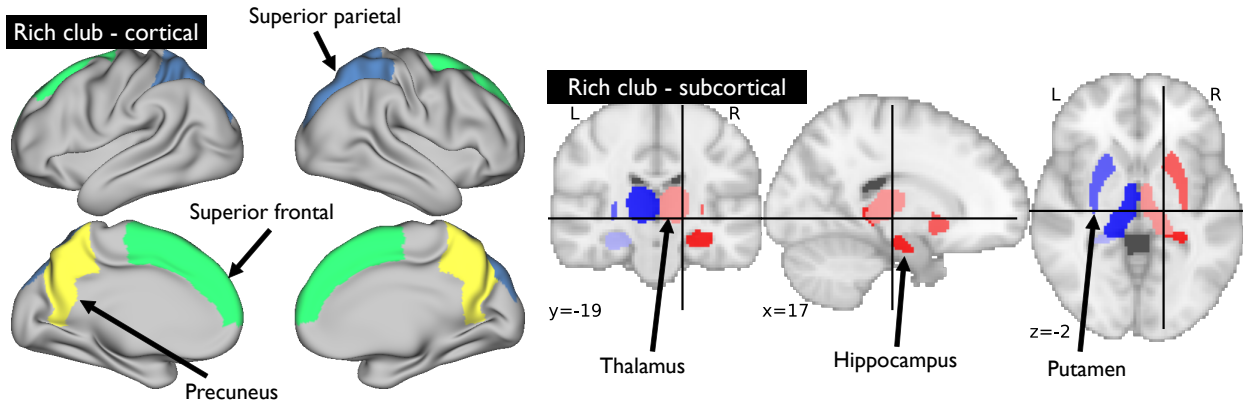

Figure 3: Visualisation of cortical (*left*) and subcortical (*right*) brain regions comprising the rich club backbone.

Network analysis of functional connectivity

Three anatomical atlases were used to define the node regions of the brain graph following preprocessing of the fMRI images, allowing us to explore reproducibility of the findings across different brain parcellations. These included the Destrieux cortical atlas (148 regions) [Fischl, 2004], the Harvard-Oxford parcellation [Desikan et al., 2006], including cortical and subcortical structures, and the AAL template (116 regions) [Tzourio-Mazoyer et al., 2002]. For each atlas and each corresponding regions, mean time series were calculated (see Fig. 2. Partial correlation between the time series was employed to estimate the strength of the functional connections, yielding a weighted graph representation [Richiardi et al., 2013]. Global efficiency of the networks was explored via the characteristic path length, L, which corresponds to the average path length $l(s)$ across all nodes s [Rubinov and Sporns, 2010]. This measure was calculated separately for positive, negative and absolute weights of the estimated partial correlation networks, as there is no consensus with regards to which of these is most discriminative.

Predictive model of functional outcome

Apart from looking at the association between the number of rich club nodes affected by stroke (N_{RC}), and the outcome measures collected at the early and late follow-ups, we devised four different predictive linear regression models. The baseline model,

$$Outcome \sim 1 + AGE + DWI_V, \tag{1}$$

is based on age and lesion volume (DWI_V) information, which have previously been identified as independent predictors of stroke outcome [Vogt et al., 2012]; [Hope et al., 2013]; [Jokinen et al., 2015]. The alternative model,

$$Outcome \sim 1 + AGE + DWI_V + N_{RC}, \tag{2}$$

incorporates N_{RC} as a cofounding factor, while the third model,

$$Outcome \sim 1 + AGE + DWI_V \times N_{RC}, \tag{3}$$

includes possible interactions between N_{RC} and DWI_V, since a positive correlation is observed between these two variables. This means that both the independent effects of N_{RC} and DWI_V and the relationship between them are taken into consideration in the linear regression model. The last model,

$$Outcome \sim 1 + AGE + DWI_V \times N_{RC} + L \times N_{RC}, \tag{4}$$

introduces the path length L and it's interaction term with N_{RC}, since targeted 'attacks' to rich club nodes have been shown to disturb global network efficiency more significantly [van den Heuvel and Sporns, 2011]. Therefore, these two predictors are expected to be related. The last model incorporates information related to how structural and functional connectivity are disrupted after stroke, and therefore can only be applied to patients with available fMRI data.

Results

Associations between functional outcome and rich club topology

We observe (Fig. 4) a positive correlation between the NIHSS assessed on early and late clinical follow-up and the number of rich club nodes affected by the acute infarct (Spearman's Rho $r_{early} = 0.54, p < 0.001$, and $r_{late} = 0.58, p = 0.001$, respectively).

We further examine the relationship between DWI volume (DWI_V) and N_{RC} to assess whether N_{RC} is determined by infarct size. As can be observed in Fig. 5, despite the positive correlation between these two measures (Spearman's Rho $r = 0.46$), there are both large infarcts that do not affect any rich club regions and small infarcts that involve one or two rich club regions; this result demonstrates that larger DWI_V does not imply greater N_{RC}.

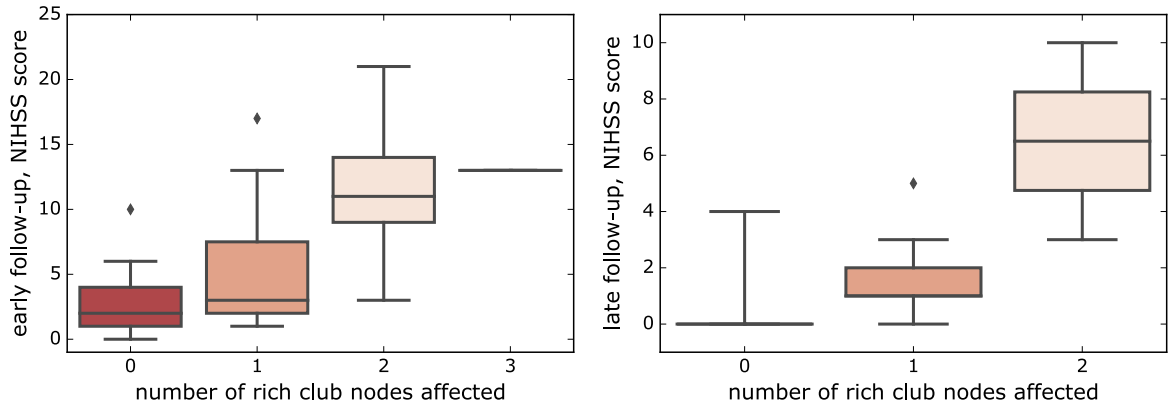

Figure 4: Early (*left*) and late (*right*) post-stroke outcome assessment in relation to the number of rich club regions affected by the stroke lesion measured on the acute MRI.

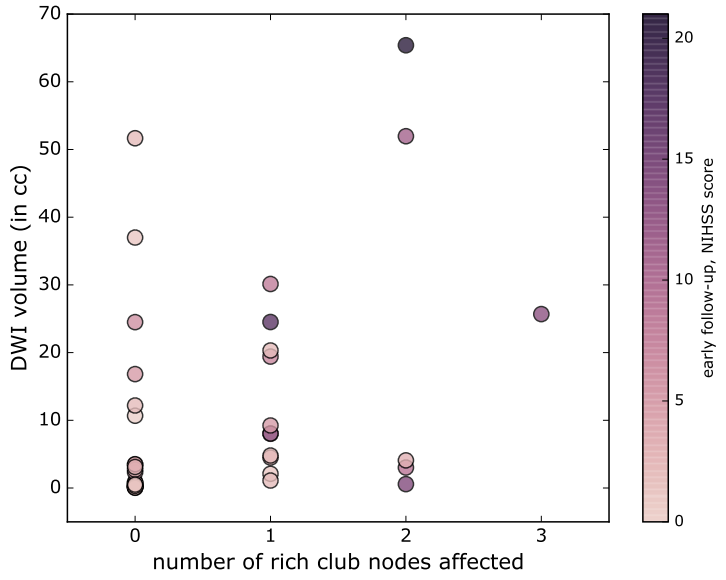

Figure 5: The association between acute infarct size, as measured by DWI volume and the number of rich club nodes affected (color-coded based on early follow-up NIHSS score).

Functional topology in the acute stroke phase

After constructing the functional connectivity networks using partial correlation, we explore the characteristic path length for positive, negative and absolute weights separately. Fig. 6 illustrates a positive correlation between the early follow-up NIHSS scores and the characteristic path length after preserving all positive connections of the functional network with nodes defined by the Harvard-Oxford atlas (Pearson's correlation coefficient $r = 0.42, p = 0.01$). A similar relationship can be observed with the AAL atlas, for which Pearson's correlation coefficient is $r = 0.38, p = 0.03$, as well as with the Destrieux atlas, with Pearson's correlation coefficient $r = 0.41, p = 0.02$. This finding could potentially indicate that the shorter the characteristic path

length in the acute phase of stroke, the more resilient the functional network is to brain damage; hence, the better the functional outcome as measured using NIHSS.

We further assessed the differences in functional network measures with respect to the 'good' or 'poor' mRS outcome. Fig. 7 demonstrates the differences identified between L for patients with 'good' (69% of patients) and 'poor' (31% of patients) outcome at 90 days post-stroke. This result is consistent across all three atlases. Our finding indicates that the characteristic path length estimated from rsfMRI scans in the acute stroke phase can be used as a predictor of functional recovery at a later stage.

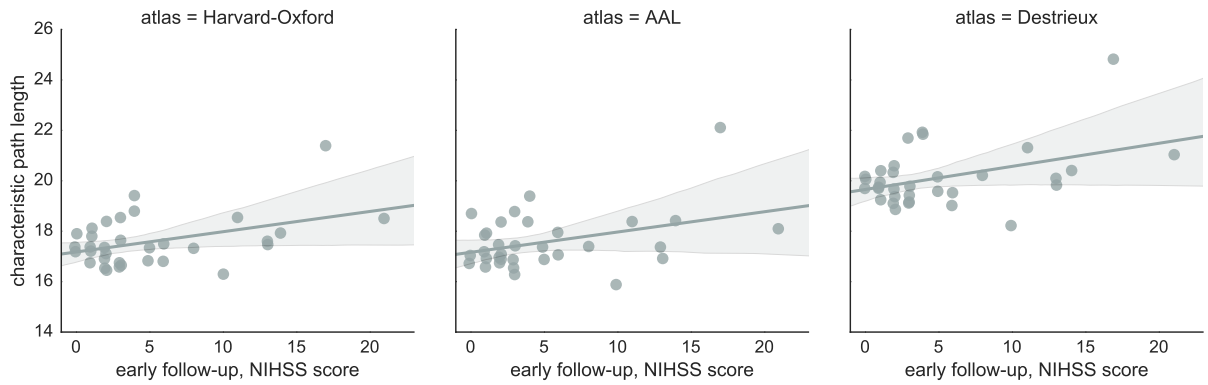

Figure 6: Characteristic path length and early follow-up NIHSS scores for three different atlases (from left to right): Harvard-Oxford (HO), Automated Anatomical Labelling (AAL), Destrieux.

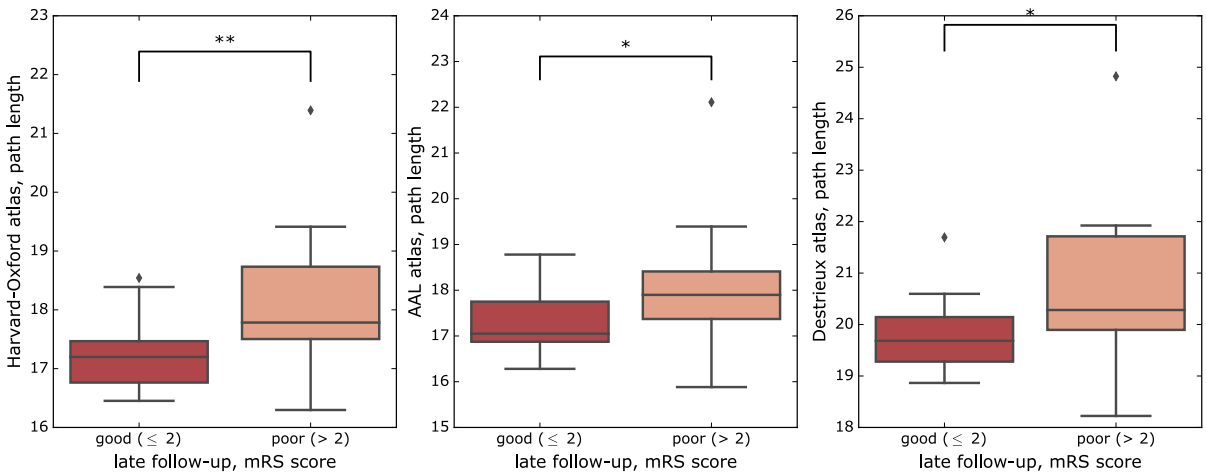

Figure 7: Characteristic path length with respect to mRS scores for three different atlases (from left to right): Harvard-Oxford (HO), Automated Anatomical Labelling (AAL), Destrieux. Definition: $mRS = 0-2$ - good outcome, $mRS = 3-6$ - poor outcome.

Table 1: Early outcome prediction model results for subjects with available fMRI data ($N = 33$). Results in parentheses correspond to all available subjects ($N = 41$).

Linear model ($NIHSS_{early} \sim$)	R^2	R^2_{adj}	p_{model}	p_{AGE}	p_{DWI_V}	$p_{N_{RC}}$
$1 + AGE + DWI_V$	0.40	0.36	4×10^{-4}	**0.01**	**0.002**	-
	(0.33)	(0.30)	(4×10^{-4})	(0.04)	(<0.001)	-
$1 + AGE + DWI_V + N_{RC}$	0.59	0.55	7×10^{-6}	0.09	0.06	**<0.001**
	(0.53)	(0.49)	(3×10^{-6})	(0.09)	(0.02)	(<0.001)
$1 + AGE + DWI_V \times N_{RC}$	0.60	0.55	2×10^{-5}	0.14	0.41	**0.03**
	(0.55)	(0.50)	(6×10^{-6})	(0.22)	(0.46)	(0.03)
$1 + AGE + DWI_V \times N_{RC} + L \times N_{RC}$	**0.69**	**0.62**	1×10^{-5}	0.26	0.59	**0.05**

Table 2: Late outcome prediction model results for subjects with available fMRI data ($N = 21$). Results in parentheses correspond to all subjects with available 90-day NIHSS scores ($N = 28$).

Linear model ($NIHSS_{late} \sim$)	R^2	R^2_{adj}	p_{model}	p_{AGE}	p_{DWI_V}	$p_{N_{RC}}$
$1 + AGE + DWI_V$	0.13	0.04	0.27	0.72	0.11	-
	(0.07)	(-0.004)	(0.40)	(0.73)	(0.18)	-
$1 + AGE + DWI_V + N_{RC}$	0.58	0.50	0.002	0.83	0.11	**<0.001**
	(0.38)	(0.30)	(0.01)	(0.82)	(0.31)	(0.002)
$1 + AGE + DWI_V \times N_{RC}$	0.60	0.50	0.004	0.96	0.07	**<0.001**
	(0.42)	(0.32)	(0.01)	(0.96)	(0.10)	(0.001)
$1 + AGE + DWI_V \times N_{RC} + L \times N_{RC}$	**0.72**	**0.60**	0.003	0.46	0.07	0.05

Predictive model based on connectivity measures

We present the results of the different linear regression models for the prediction of early and late functional post-stroke outcome in terms of explained variance (R^2 and R^2_{adj}) and statistical significance in Tables 1 and 2, respectively. Model 3 outperforms model 1, with $R^2 = 0.60$ for both the early and late outcome.

Importantly, the estimated coefficient of this model for N_{RC} is significant ($\beta_{early} = 2.79, p = 0.03$ for the early and $\beta_{late} = 3.25, p < 0.001$ for the late outcome), while this is not the case for DWI_V and AGE after including the interaction term. Model metrics improve further after introducing the path length (L) as a measure of network efficiency and its interaction term with N_{RC} in model 4, yielding $R^2 = 0.69$ for the early outcome prediction and $R^2 = 0.72$ for the late outcome (a 5-fold increase over the baseline model), while N_{RC} remains statistically significant for the early outcome.

Additionally, the linear regression models are compared by means of two commonly used information criteria, i.e. Akaike information criterion (AIC) [Akaike, 1974] and Bayes information criterion (BIC) [Stone, 1979], in Table 3. It should be noted that the model with the lowest information criterion value is considered the best-fitting model. As can be observed, model 4 is the best-fitting one according to AIC, for both early and late outcomes. BIC, however, which measures the trade-off between model fit and complexity of the model, slightly favours model 2 (4 estimated parameters), which is much less complex than model 4 (7 estimated parameters). For both outcomes and information criteria, though, there is a drastic improvement of the model fit compared to model 1, which disregards connectivity measures.

Table 3: Information criteria for model comparison.

Linear model ($NIHSS \sim$)	AIC_{early}	BIC_{early}	AIC_{late}	BIC_{late}
$1 + AGE + DWI_V$	192.07	196.56	99.56	102.70
$1 + AGE + DWI_V + N_{RC}$	181.45	**187.43**	86.54	**90.72**
$1 + AGE + DWI_V \times N_{RC}$	182.64	190.12	87.20	92.43
$1 + AGE + DWI_V \times N_{RC} + L \times N_{RC}$	**178.49**	188.96	**84.14**	91.45

Discussion

We explored the importance of the integrity of the rich club backbone on functional outcomes after AIS, as well as the topology of functional networks obtained with different anatomical atlases. Functional outcomes vary significantly in the early and late phase of stroke recovery and are difficult to predict at AIS onset. Using the acute stroke lesions visible on the admission DWI, we determined that the greater the number of rich club nodes affected by the stroke lesion is, the worse the functional outcome, both when assessed early (2-5 days) and late (90-days) post-stroke. Importantly, this association was independent of age and infarct volume. Our findings align with a previous report [Munsch et al., 2015], which identified stroke location as an independent predictor of cognitive outcome as measured at 3 months post-stroke. Similar results were demonstrated by [Wu et al., 2015], highlighting the importance of joint modelling of DWI volume and topography for stroke outcomes, while our approach also takes network topology into account.

Rich club nodes comprise brain areas responsible for distributing a large fraction of the brain's neural communications. This underpins the importance of these brain regions for recovery after brain damage, as local disruptions to these central hubs of information flow most likely affect the brain more severely at a global level. The predictive model was further improved after introducing a measure of functional network efficiency, as measured by the network's characteristic path length, which directly describes how focal lesions affect the brain network at a global level. Furthermore, our results suggest that a reduced path length could facilitate recovery or make the brain less vulnerable to damage.

These data underscore the importance of efficient brain connectivity in functional recovery and resilience to brain damage after ischemic stroke. Our model accounts for some of the most commonly reported confounding factors that are available in the acute setting, i.e. age [Saposnik et al., 2012]; [Rost et al., 2016] and lesion volume [Vogt et al., 2012] as measured on the acute DWI image. Our results indicate that infarct location improves the model independent of infarct size, which has been previously suggested by [Wu et al., 2015] in a study of infarct topography. We found that, although the number of rich club nodes affected by the infarct is correlated with the DWI lesion volume, the volume alone is not enough to explain the early and late outcomes as measured by the NIHSS score.

We further explored how focal lesions affect functional brain connectivity at a global level in the acute stroke phase, and whether network measures can be used to reflect the brain's resilience to damage and potentially facilitate recovery. We observed a statistically significant positive correlation between the characteristic path length and early functional outcome. We, further, reported significant differences between good and poor outcome, as determined by dichotomizing mRS and L, which could indicate that the brain may benefit from a low characteristic path length with regards to facilitating recovery. Nevertheless, the assumption of direct causation between these two measures needs to be carefully explored.

There are certain limitations that need to be taken into consideration when interpreting these results. First, regional delays have been identified in rsfMRI fluctuations in stroke and cerebrovascular disease patients (hemodynamic lag), which takes place due to vascular occlusion [Siegel et al., 2017]. These delays are

measured by time shift analysis of regional BOLD time series with respect to a reference signal. Approaches have been proposed to correct for lags in FC analysis, such as shifting the time series in the lagged tissues prior to the estimation of functional connectivity [Siegel et al., 2016]. However, there is no consensus on how such lags should be accounted for. Importantly, the effect of hemodynamic lag and the subsequent drop in the estimated FC are an integral part of the observed differences between patients, and may be utilized to determine variations in outcome. Another limitation that should be taken into account results from potential registration errors, due to relatively low through-plane resolution of the anatomical scans and the fact that the lesions were not masked out when registering the anatomical scans to the MNI template. Among the strengths of this study is the thoroughly ascertained and well-characterized hospital-based dataset of patients with AIS and consecutive assessments of functional post-stroke outcomes.

Overall, this is the first study exploring functional network topology and rich club topology of brain connectivity in AIS patients, as well as their association with early and late post-stroke outcomes. Our findings highlight the impact of stroke location on functional recovery and the importance of structural connectivity hubs and functional connectivity integration for efficient information transmission underlying the mechanisms of stroke recovery. The proposed model yields a remarkable 5-fold improvement in explained variance over the baseline model, based on age and lesion volume.

Acknowledgements

This work was funded by NIH Grant 5R01NS082285. Sofia Ira Ktena was supported by the EPSRC Centre for Doctoral Training in High Performance Embedded and Distributed Systems (HiPEDS, Grant Reference EP/L016796/1) and an EMBO short-term fellowship (Reference 7284). Markus D. Schirmer was supported by the European Union's Horizon 2020 research and innovation programme under the Marie Sklodowska-Curie grant agreement No 753896.

References

Feigin VL, Forouzanfar MH, Krishnamurthi R, Mensah GA, Connor M, Bennett DA, Moran AE, Sacco RL, Anderson L, Truelsen T, O'Donnell M, Venketasubramanian N, Barker-Collo S, Lawes CMM, Wang W, Shinohara Y, Witt E, Ezzati M, Naghavi M, Murray C (2014): Global and regional burden of stroke during 1990–2010: findings from the Global Burden of Disease Study 2010. The Lancet 383:245–255. https://doi.org/10.1016%2Fs0140-6736%2813%2961953-4.

Carlo AD (2008): Human and economic burden of stroke. Age and Ageing 38:4–5. https://doi.org/10.1093%2Fageing%2Fafn282.

Counsell C, Dennis M (2001): Systematic Review of Prognostic Models in Patients with Acute Stroke. Cerebrovascular Diseases 12:159–170. https://doi.org/10.1159%2F000047699.

Kent TA, Soukup VM, Fabian RH (2001): Heterogeneity Affecting Outcome From Acute Stroke Therapy: Making Reperfusion Worse. Stroke 32:2318–2327. https://doi.org/10.1161%2Fhs1001.096588.

Meschia JF (2002): Addressing the Heterogeneity of the Ischemic Stroke Phenotype in Human Genetics Research. Stroke 33:2770–2774. https://doi.org/10.1161%2F01.str.0000035261.28528.c8.

Muir KW (2002): Heterogeneity of Stroke Pathophysiology and Neuroprotective Clinical Trial Design. Stroke 33:1545–1550. https://doi.org/10.1161%2F01.str.0000018684.86293.ab.

Etherton MR, Wu O, Cougo P, Giese A-K, Cloonan L, Fitzpatrick KM, Kanakis AS, Boulouis G, Karadeli HH, Lauer A, Rosand J, Furie KL, Rost NS (2017): Integrity of normal-appearing white matter and functional outcomes after acute ischemic stroke. Neurology 88:1701–1708. https://doi.org/10.1212%2Fwnl.0000000000003890.

Rubinov M, Sporns O (2010): Complex network measures of brain connectivity: Uses and interpretations. NeuroImage 52:1059–1069. https://doi.org/10.1016%2Fj.neuroimage.2009.10.003.

Heuvel MP van den, Sporns O (2011): Rich-Club Organization of the Human Connectome. Journal of Neuroscience 31:15775–15786. https://doi.org/10.1523%2Fjneurosci.3539-11.2011.

Chung AW, Schirmer MD, Krishnan ML, Ball G, Aljabar P, Edwards AD, Montana G (2016): Characterising brain network topologies: A dynamic analysis approach using heat kernels. NeuroImage 141:490–501. https://doi.org/10.1016%2Fj.neuroimage.2016.07.006.

Ktena SI, Parisot S, Passerat-Palmbach J, Rueckert D (2016): Comparison of brain networks with unknown correspondences. arXiv preprint arXiv:161104783.

Fornito A, Zalesky A, Breakspear M (2015): The connectomics of brain disorders. Nature Reviews Neuroscience 16:159–172. https://doi.org/10.1038%2Fnrn3901.

Kawahara J, Brown CJ, Miller SP, Booth BG, Chau V, Grunau RE, Zwicker JG, Hamarneh G (2017): BrainNetCNN: Convolutional neural networks for brain networks: towards predicting neurodevelopment. NeuroImage 146:1038–1049. https://doi.org/10.1016%2Fj.neuroimage.2016.09.046.

Ktena SI, Parisot S, Ferrante E, Rajchl M, Lee M, Glocker B, Rueckert D (2018): Metric learning with spectral graph convolutions on brain connectivity networks. NeuroImage 169:431–442. https://doi.org/10.1016%2Fj.neuroimage.2017.12.052.

Achard S (2006): A Resilient Low-Frequency, Small-World Human Brain Functional Network with Highly Connected Association Cortical Hubs. Journal of Neuroscience 26:63–72. https://doi.org/10.1523%2Fjneurosci.3874-05.2006.

Joyce KE, Hayasaka S, Laurienti PJ (2013): The Human Functional Brain Network Demonstrates Structural and Dynamical Resilience to Targeted Attack. Ed. by Sophie Achard. PLoS Computational Biology 9:e1002885. https://doi.org/10.1371%2Fjournal.pcbi.1002885.

Lo C-YZ, Su T-W, Huang C-C, Hung C-C, Chen W-L, Lan T-H, Lin C-P, Bullmore ET (2015): Randomization and resilience of brain functional networks as systems-level endophenotypes of schizophrenia. Proceedings of the National Academy of Sciences 112:9123–9128. https://doi.org/10.1073%2Fpnas.1502052112.

Raj A, Kuceyeski A, Weiner M (2012): A Network Diffusion Model of Disease Progression in Dementia. Neuron 73:1204–1215. https://doi.org/10.1016%2Fj.neuron.2011.12.040.

Deco G, Tononi G, Boly M, Kringelbach ML (2015): Rethinking segregation and integration: contributions of whole-brain modelling. Nature Reviews Neuroscience 16:430–439. https://doi.org/10.1038%2Fnrn3963.

Heuvel MP van den, Sporns O, Collin G, Scheewe T, Mandl RCW, Cahn W, Goñi J, Pol HEH, Kahn RS (2013): Abnormal Rich Club Organization and Functional Brain Dynamics in Schizophrenia. JAMA Psychiatry 70:783. https://doi.org/10.1001%2Fjamapsychiatry.2013.1328.

Wu O, Cloonan L, Mocking SJT, Bouts MJRJ, Copen WA, Cougo-Pinto PT, Fitzpatrick K, Kanakis A, Schaefer PW, Rosand J, Furie KL, Rost NS (2015): Role of Acute Lesion Topography in Initial Ischemic Stroke Severity and Long-Term Functional Outcomes. Stroke 46:2438–2444. https://doi.org/10.1161%2Fstrokeaha.115.009643.

Munsch F, Sagnier S, Asselineau J, Bigourdan A, Guttmann CR, Debruxelles S, Poli M, Renou P, Perez P, Dousset V, Sibon I, Tourdias T (2015): Stroke Location Is an Independent Predictor of Cognitive Outcome. Stroke 47:66–73. https://doi.org/10.1161%2Fstrokeaha.115.011242.

Jokinen H, Melkas S, Ylikoski R, Pohjasvaara T, Kaste M, Erkinjuntti T, Hietanen M (2015): Post-stroke cognitive impairment is common even after successful clinical recovery. European Journal of Neurology 22:1288–1294. https://doi.org/10.1111%2Fene.12743.

Vogt G, Laage R, Shuaib A, and AS (2012): Initial Lesion Volume Is an Independent Predictor of Clinical Stroke Outcome at Day 90: An Analysis of the Virtual International Stroke Trials Archive (VISTA) Database. Stroke 43:1266–1272. https://doi.org/10.1161%2Fstrokeaha.111.646570.

Hope TMH, Seghier ML, Leff AP, Price CJ (2013): Predicting outcome and recovery after stroke with lesions extracted from MRI images. NeuroImage: Clinical 2:424–433. https://doi.org/10.1016%2Fj.nicl.2013.03.005.

Park C-h., Chang WH, Ohn SH, Kim ST, Bang OY, Pascual-Leone A, Kim Y-H (2011): Longitudinal Changes of Resting-State Functional Connectivity During Motor Recovery After Stroke. Stroke 42:1357–1362. https://doi.org/10.1161%2Fstrokeaha.110.596155.

Golestani A-M, Tymchuk S, Demchuk A, and BGG (2012): Longitudinal Evaluation of Resting-State fMRI After Acute Stroke With Hemiparesis. Neurorehabilitation and Neural Repair 27:153–163. https://doi.org/10.1177%2F1545968312457827.

Carter AR, Astafiev SV, Lang CE, Connor LT, Rengachary J, Strube MJ, Pope DL, Shulman GL, Corbetta M (2010): Resting interhemispheric functional magnetic resonance imaging connectivity predicts performance after stroke.. Ann Neurol 67:365–75.

Rehme AK, Grefkes C (2013): Cerebral network disorders after stroke: evidence from imaging-based connectivity analyses of active and resting brain states in humans.. J Physiol 591:17–31.

Fazekas F, Chawluk JB, Alavi A, Hurtig HI, Zimmerman RA (1987): MR signal abnormalities at 1.5 T in Alzheimer's dementia and normal aging. American Journal of Roentgenology 149:351–356. https://doi.org/10.2214%2Fajr.149.2.351.

Neurological Disorders TNI of, Stroke Study Group S rt-PA (1995): Tissue Plasminogen Activator for Acute Ischemic Stroke. New England Journal of Medicine 333:1581–1588. https://doi.org/10.1056%2Fnejm199512143332401.

Cumming TB, Blomstrand C, Bernhardt J, Linden T (2010): The NIH Stroke Scale Can Establish Cognitive Function after Stroke. Cerebrovascular Diseases 30:7–14. https://doi.org/10.1159%2F000313438.

Rankin J (1957): Cerebral Vascular Accidents in Patients over the Age of 60: I. General Considerations. Scottish Medical Journal 2:127–136. https://doi.org/10.1177%2F003693305700200401.

Bloch RF (1988): Interobserver agreement for the assessment of handicap in stroke patients.. Stroke 19:1448–1448. https://doi.org/10.1161%2F01.str.19.11.1448.

Wilson JTL, Hareendran A, Hendry A, Potter J, Bone I, Muir KW (2005): Reliability of the Modified Rankin Scale Across Multiple Raters. Stroke 36:777–781. https://doi.org/10.1161%2F01.str.0000157596.13234.95.

Banks JL, Marotta CA (2007): Outcomes Validity and Reliability of the Modified Rankin Scale: Implications for Stroke Clinical Trials: A Literature Review and Synthesis. Stroke 38:1091–1096. https://doi.org/10.1161%2F01.str.0000258355.23810.c6.

Quinn TJ, Dawson J, Walters MR, Lees KR (2009): Reliability of the Modified Rankin Scale: A Systematic Review. Stroke 40:3393–3395. https://doi.org/10.1161%2Fstrokeaha.109.557256.

Cameron C, Sharad S, Brian C, Ranjeet K, Satrajit G, Chaogan Y, Qingyang L, Daniel L, Joshua V, Randal B, Stanley C, Maarten M, Clare K, Adriana DM, Francisco C, Michael M (2013): Towards Automated Analysis of Connectomes: The Configurable Pipeline for the Analysis of Connectomes (C-PAC). Frontiers in Neuroinformatics 7. https://doi.org/10.3389%2Fconf.fninf.2013.09.00042.

Tustison NJ, Avants BB, Cook PA, Gee JC (2010): N4ITK: Improved N3 bias correction with robust B-spline approximation. In: . 2010 IEEE International Symposium on Biomedical Imaging: From Nano to Macro. IEEE. https://doi.org/10.1109%2Fisbi.2010.5490078.

Avants BB, Tustison NJ, Song G, Cook PA, Klein A, Gee JC (2011): A reproducible evaluation of ANTs similarity metric performance in brain image registration. NeuroImage 54:2033–2044. https://doi.org/10.1016%2Fj.neuroimage.2010.09.025.

Woolrich MW, Jbabdi S, Patenaude B, Chappell M, Makni S, Behrens T, Beckmann C, Jenkinson M, Smith SM (2009): Bayesian analysis of neuroimaging data in FSL. NeuroImage 45:S173–S186. https://doi.org/10.1016%2Fj.neuroimage.2008.10.055.

Smith SM (2002): Fast robust automated brain extraction. Human Brain Mapping 17:143–155. https://doi.org/10.1002%2Fhbm.10062.

Desikan RS, Ségonne F, Fischl B, Quinn BT, Dickerson BC, Blacker D, Buckner RL, Dale AM, Maguire RP, Hyman BT, Albert MS, Killiany RJ (2006): An automated labeling system for subdividing the human cerebral cortex on MRI scans into gyral based regions of interest. NeuroImage 31:968–980. https://doi.org/10.1016%2Fj.neuroimage.2006.01.021.

Fischl B (2004): Automatically Parcellating the Human Cerebral Cortex. Cerebral Cortex 14:11–22. https://doi.org/10.1093%2Fcercor%2Fbhg087.

Tzourio-Mazoyer N, Landeau B, Papathanassiou D, Crivello F, Etard O, Delcroix N, Mazoyer B, Joliot M (2002): Automated Anatomical Labeling of Activations in SPM Using a Macroscopic Anatomical Parcellation of the MNI MRI Single-Subject Brain. NeuroImage 15:273–289. https://doi.org/10.1006%2Fnimg.2001.0978.

Richiardi J, Achard S, Bunke H, Ville DVD (2013): Machine Learning with Brain Graphs: Predictive Modeling Approaches for Functional Imaging in Systems Neuroscience. IEEE Signal Processing Magazine 30:58–70. https://doi.org/10.1109%2Fmsp.2012.2233865.

Akaike H (1974): A New Look at the Statistical Model Identification. In: . Springer Series in Statistics. Springer New York. pp 215–222. https://doi.org/10.1007%2F978-1-4612-1694-0_16.

Stone M (1979): Comments on Model Selection Criteria of Akaike and Schwarz. Journal of the Royal Statistical Society Series B (Methodological) 41.

Saposnik G, Guzik AK, Reeves M, Ovbiagele B, Johnston SC (2012): Stroke Prognostication using Age and NIH Stroke Scale: SPAN-100. Neurology 80:21–28. https://doi.org/10.1212%2Fwnl.0b013e31827b1ace.

Rost NS, Bottle A, Lee J-M, Randall M, Middleton S, Shaw L, Thijs V, Rinkel GJE, and TMH (2016): Stroke Severity Is a Crucial Predictor of Outcome: An International Prospective Validation Study. Journal of the American Heart Association 5. https://doi.org/10.1161%2Fjaha.115.002433.

Siegel JS, Shulman GL, Corbetta M (2017): Measuring functional connectivity in stroke: Approaches and considerations. Journal of Cerebral Blood Flow & Metabolism 37:2665–2678. https://doi.org/10.1177%2F0271678x17709198.

Siegel JS, Snyder AZ, Ramsey L, Shulman GL, Corbetta M (2016): The effects of hemodynamic lag on functional connectivity and behavior after stroke. Journal of Cerebral Blood Flow & Metabolism 36:2162–2176. https://doi.org/10.1177%2F0271678x15614846.